ISJ 7: 89-106, 2010 ISSN 1824-307X

RESEARCH REPORT

The effect of oxidative stress on phagocytosis and apoptosis in the earthworm *Eisenia hortensis*

SL Fuller-Espie, T Nacarelli, EL Blake, FM Bearoff

Science Department, Cabrini College, 610 King of Prussia Road, Radnor, Pennsylvania 19087-3698, USA

Accepted February 17, 2010

Abstract

The effect of exogenous hydrogen peroxide (H_20_2) on phagocytic function and apoptosis in coelomocytes from *Eisenia hortensis* was investigated. Treating coelomocytes with H_20_2 (0.26 to 8.4 mM) evoked a significant increase in phagocytosis for one or more of the concentrations of H_20_2 employed in 67 % of cases. Using annexin V-FITC we show that H_20_2 induced apoptosis of coelomocytes *in vitro*. We found that 100 % of viable coelomocyte populations exhibited significant increases in phosphatidylserine translocation for one or more of the concentrations of H_20_2 tested (8.4 to 67.6 mM). Using a fluorescent inhibitor of caspases, we revealed the presence of activated caspases observing increased caspase activity in 67 % of viable coelomocyte populations treated with 33.8mM H_20_2, and in 100 % of cases treated with 67.6 mM H_20_2. Agarose gel electrophoresis and the TUNEL assay showed DNA fragmentation in samples treated with 16.9 and 33.8 mM H_20_2. In addition, endogenous H_20_2 production during phagocytosis by hyaline amoebocytes was detected using a fluorogenic substrate. Thus, free radicals not only appear to facilitate phagocytosis and are produced during phagocytosis, but they also promote an oxidative-stress-induced apoptosis that may play an important function in regulating innate immune responses in *E. hortensis*.

Key Words: phagocytosis; hydrogen peroxide; annexin V; DNA fragmentation; caspase, TUNEL assay

Introduction

When the production of reactive oxygen species (ROS) in microsomes, peroxisomes, mitochondria and the cytosol overwhelms a cell's ability to either neutralize reactive intermediates or repair toxic effects from ROS, a state of oxidative stress is initiated. Toxic effects from ROS include damage to nucleic acids (mutagenesis) and carbohydrates, lipid peroxidation of cellular membranes, and enzyme inactivation (Imlay, 2003). Oxidative stress is also linked to the aging process (Larsen, 1993; Helfand and Rogina, 2003; Rattan, 2006; Csiszar *et al.,* 2007). ROS encompass a wide array of oxidants including hydrogen peroxide (H_20_2, the focus of this study), superoxide anions, hydroxyl radicals, peroxyl radicals and organic hydroperoxides (Dunford, 1987; Coffey *et al.*, 1995; Panasenko *et al.*, 2002). These oxidants are produced through various means including radiation, uncomplexed metals such as iron and copper, organic compounds such as quinones, uric acid and homocysteines, certain classes of xenobiotics such as polycyclic aromatic hydrocarbons (PAH) going through redox cycling, and thermal stress (DiGuilioi *et al.,* 1989; Livingstone *et al.,* 1990; Sundaram *et al.,* 1990; Livingstone *et al.,* 1995; Abele *et al.,* 2001; Tyagi *et al.,* 2005; Valko *et al.,* 2006; Strazzullo and Puig, 2007; Fato *et al.,* 2008; Pichaud *et al.,* 2008; Kell, 2009). They are also generated by intracellular enzymes including NADPH oxidase, xanthine oxidase and cytochrome P450 (Lewis, 2002; Bedard and Krause, 2007; Jankov *et al.,* 2008). Paradoxically, ROS not only exert damaging effects in cells, but they also afford protecive effects, for example during immune defense for phagocytosis where ROS are toxic to phagocytized pathogens. Another benefit of ROS is their aility to participate in redox signaling (Thannickal and Fanburg, 2000; Forman and Torres, 2002; Wang, 2009).

Because of the detrimental effects of ROS on cellular components, it is imperative that organisms possess cellular antioxidant defense mechanisms for the detoxification of ROS, often measured as the total oxyradical scavenging capacity (TOSC), an important biomarker of oxidative stress (Regoli, 2000; Gorbi and Regoli, 2003; Dovzhenko *et al.,* 2005). ROS are neutralized by a variety of

Corresponding author:
SL Fuller-Espie
Science Department
Cabrini College
610 King of Prussia Road, Radnor, PA 19087-3698, USA
Email: sfuller-espie@cabrini.edu

antioxidant processes aimed at stabilizing free radicals, terminating free radical reactions, and preventing the transfer of electrons from oxygen to organic molecules. One mechanism relies upon enzymatic detoxification of ROS by catalase, glutathione peroxidase, superoxide dismutase, thioredoxin reductase, peroxiredoxins and sulfiredoxin (Raes *et al.,* 1994; Nordberg and Arnér, 2001; Flohé *et al.,* 2003; Findlay *et al.,* 2005). Nonenzymatic antioxidants also provide antioxidant defenses and include a diverse array of molecules including antioxidant quenchers comprising cellular proteins (e.g. transferrin, ferritin, metallothionein, ceruplasmin and others) that chelate pro-oxidant minerals (Cairo *et al.,* 1995; Kang *et al.,* 2001; Yamaji *et al.,* 2004; Laukens *et al.,* 2009). In addition, glutathione, selenium, phytochemicals, vitamin E, vitamin C and provitamin A compounds (e.g. beta carotene) also provide protective antioxidant defenses (Sies *et al.,* 1992; Loo, 2003; Brenneisen *et al.,* 2005; Ghezzi, 2005).

The primary goal of this study was to investigate the *in vitro* effects of oxidative stress on cellular activities in the immune cells (coelomocytes) of the earthworm *Eisenia hortensis* (also known as the European nightcrawler) which reside in the coelomic cavity. Investigations of innate immunity in earthworms have identified three distinct subpopulations of coelomocytes (leukocyte equivalents): hyaline amoebocytes (large coelomocytes), granular amoebocytes (small coelomocytes) and chloragocytes (eleocytes), most likely diverging developmentally from a common progenitor cell (prohemocyte), as suggested by Hartenstein (2006). The immune functions of coelomocytes can be studied *in vitro* after harvesting the coelomic fluid, which is rich in coelomocytes, by extruding the coelomocytes through the dorsal pores of the body wall from experimentally-induced earthworms. The hyaline amoebocytes are the major phagocytic cells, the granular amoebocytes constitute the subpopulation exhibiting NK-like activity, and the eleocytes contain chloragosomes and do not participate in either phagocytic or NK-like activities, but they do secrete lytic substances (Cooper, 1996; Cossarizza *et al.,* 1996; Adamowicz and Wojtaszek, 2001; Engelmann *et al.,* 2002; Engelmann *et al.,* 2005). Differences in granularity and size between coelomocytes permits amoebocytes (hyaline and granular) and eleocytes to be distinguished using flow cytometry methodology employing forward light scatter (FSC) and side light scatter (SSC) measurements (Cossarizza *et al.,* 1996, 2005; Engelmann *et al.,* 2004; Patel *et al.,* 2007; Fuller-Espie *et al.,* 2008). Selective analysis of subpopulations is facilitated by specifying regions to identify particular subpopulations, and then gating on assigned regions, permitting the investigator to include only desired subpopulations and exclude irrelevant subpopulations from final analyses. Light and fluorescent microscopy have been used by researchers to study immune functions in earthworms (Adamowicz and Wojtaszek, 2001; Kalaç *et al*., 2002), however, these methods are more subjective than flow cytometry, and they impose restrictions on the number of cells included in analyses owing to time constraints. In contrast, flow cytometry is an objective, quantitative methodology that analyzes thousands of cells per second with the option of restricting analyses to predetermined subpopulations.

This investigation focused specifically on phagocytic function and the induction of apoptosis in the amoebocytes of *E. hortensis* following exposure to exogenous H_20_2. We evaluated the phagocytic uptake of *Escherichia coli* using flow cytometry and found that *in vitro* exposure to H_20_2 (0.26 - 8.4 mM) enhanced phagocytosis. Using flow cytometric and agarose gel electrophoresis methodologies we also examined the effect of H_20_2 on three events associated with apoptosis: 1) translocation of phosphatidylserine (PS) to the extracellular face of the plasma membrane using annexin-V binding; 2) caspase activation using a fluorescein-conjugated inhibitor of caspase activation (FLICA); and 3) DNA fragmentation. We present data supporting an apoptotic-like cell death in coelomocytes of *E. hortensis* resulting from *in vitro* exposure to exogenous H_20_2 (8.4 - 67.6 mM). Finally, using the fluorogenic substrate DHR 123, a probe widely used to measure intracellular H_20_2, we also show that H_20_2 is generated in hyaline amoebocytes during phagocytosis of *Bacillus megaterium* and *Pseudomonas stutzeri*.

Materials and Methods

Cell culture supplies and chemical reagents

Tissue culture plasticware was purchased from Fisher Scientific. Phosphate buffered saline (PBS) was purchased from Invitrogen. Dulbecco's Modified Eagle Medium (DMEM, Invitrogen) was supplemented with either 10 % heat-inactivated fetal calf serum (Invitrogen) or Serum Supreme (Lonza BioWhittaker), plus 100 μg ml^{-1} ampicillin (Shelton Scientific), 10 μg ml^{-1} kanamycin (Shelton Scientific), 10 μg ml^{-1} tetracycline, 5 μg ml^{-1} chloramphenicol (Fluka Biochemika), 1× penicillin, streptomycin and amphotericin B, 1× nonessential amino acids (Invitrogen) and 1× L-glutamine (Invitrogen) to comprise Super DMEM (SDMEM). SDMEM supplemented with Serum Supreme was used for all exogenous H_20_2 assays while SDMEM supplemented with fetal calf serum was used for endogenous H_20_2 assays.

Earthworm husbandry

Eisenia hortensis (European nightcrawlers) was purchased from Vermitechnology Unlimited, Orange Lake, Florida, USA, who imports *E. hortensis* from Star Food, Holland, Scherpenzeelseweg 95, 3772ME Barneveld, The Netherlands. Species identity was determined by the United States Department of Agriculture, USDA Permit #52262 (Vermitechnology, personal communication). Short-term colonies were maintained at RT in the dark on moistened autoclaved pine woodchips sprinkled with Single Grain Rice Cereal or Rice with Bananas Cereal (Gerber) and covered with autoclaved, shredded and moistened paper towels. Habitats were changed twice weekly. Animals were euthanized by freezing at -20 ^{o}C.

Extrusion of coelomocytes

Prior to experimentation, earthworms were first washed with distilled water on paper towels using a water bottle to remove wood chip fragments or food particles. They were then placed overnight on paper towels moistened with 2.5 μg ml^{-1} Fungizone (Fisher Scientific) in 100 mm Petri dishes to minimize fecal contamination during the extrusion process, and remove further any surface contaminants. To collect coelomocytes, earthworms were placed in either 100 mm Petri dishes or in multichannel pipette reservoirs containing 3 ml BD FACSFlow sheath fluid (BD Biosciences). The earthworms extruded their coelomocytes through their dorsal pores in response to this external stimulus without the need to use the alcohol extrusion method reported by others (Engelmann et al., 2005). The coelomocytes were then transferred to 0.5 ml Accumax (Innovative Cell Technology) in 15 ml conical test tubes for a 5 min incubation period at RT to reduce aggregation of cells. Finally, 5 ml PBS was added and the samples were centrifuged immediately at 150 x g, 5 min at 4 ^{o}C. After decanting the supernatant, the coelomocyte pellet was gently mixed by flicking the bottom of the centrifuge tube, and coelomocytes were resuspended in 0.5 ml SDMEM. Enumeration was carried out using a hemacytometer. Only hyaline amoebocytes (large coelomocytes) and hyaline granulocytes (small coelomocytes) were included in the cell count; eleocytes were not counted but did factor into a quality score. Samples with large numbers of eleocytes compared to large and small coelomocytes were not used in phagocytosis assays. Samples were adjusted to 3.8 x 10^5 or 5 x 10^5 (phagocytosis and annexin V assays, see below) or 1 x 10^6 (caspase assays) coelomocytes ml^{-1} in SDMEM.

Bacteria for phagocytosis assays

E. coli/GFP: *Escherichia coli* HB101 transformed with pGLO (BioRad) and expressing green fluorescent protein (GFP) were grown on tryptic soy agar containing 100 μg ml^{-1} ampicillin and 0.2 % (w/v) arabinose at 32 °C for 24 h. After washing the cells once in PBS, they were fixed chemically with 4 % (v/v) paraformaldehyde in PBS, 1 h at RT with periodic mixing, followed by three PBS washes. Centrifugation was carried out at 3273x*g* for 5 min at 4 ^{o}C. The final cell pellet was resuspended in PBS, bacteria were enumerated using a hemacytometer, and then stored in the dark at 4 °C.

Bacillus megaterium and *Pseudomonas stutzeri* (Presque Isle Cultures) were grown overnight in tryptic soy broth at 37 ^{o}C in a shaking incubator. Absorbance was measured using a spectrophotometer (600 nm) and compared to a standard curve to determine concentration. Standard curves were generated by correlating absorbance with cell count using a hemacytometer.

All bacteria were diluted in SDMEM to obtain the desired multiplicity of infection (m.o.i.).

Phagocytosis: exogenous H_20_2 pretreatment

Phagocytosis assays were carried out in SDMEM. Coelomocytes (50,000 per well) were pretreated with or without H_20_2 (0 - 8.4 mM final concentration) 5 % CO_2, at 25 ^{o}C in 96-well, round-bottom plates in 200 μl SDMEM. Duplicate samples were used in every assay. Following H_20_2 pretreatment, cells were centrifuged (150x*g*) and washed once with PBS. Finally, 200 μl *E. coli*/GFP was added to each well at a multiplicity of infection of 1000 bacteria:1 coelomocyte and incubated for 3 h at 30 °C. To control for non-specific binding of *E. coli*/GFP to the external surface of coelomocytes, 50 μM cytochalasin B (Sigma Aldrich) [an antibiotic that interferes with microfilament activity and thereby inhibits phagocytosis (Axline and Reaven, 1974)] was added to control wells 45 min before the addition of *E.coli*/GFP.

Following *E. coli*/GFP uptake, trypan blue (BioWhittaker) was used at a final concentration of 0.02 % (w/v) for 30 min at RT in the dark, for quenching purposes to reduce background fluorescence (Mosiman *et al.,* 1997). The cells were transferred to flow cytometry tubes containing 100 μl FACS Flow buffer (BD Biosciences), placed on ice in the dark, and run immediately on the flow cytometer.

Annexin V-FITC/PI assay

Recombinant human annexin V-FITC (Invitrogen, ANNEXINV01)) and propidium iodide (PI) (Invitrogen, P3566) were used to detect PS translocation and to enable exclusion of dead cells from analyses. Using a 96-well, round-bottom plate, 5 x 10^4 (assay 1) or 3.8 x 10^4 (assay 2) coelomocytes in 50 μl SDMEM were added to appropriate experimental (H_20_2-treated) and control (double negative autofluorescent background; single positive FITC; single positive PI; double positive annexin V/PI background) wells in triplicate. Experimental wells received 50 μl of H_20_2 (final concentrations of 67.6, 33.8, 16.9, and 8.45 mM). Single positive FITC controls received 50 μl of H_20_2 (270mM final). Single positive PI controls received 50 μl saponin (0.01 % final). The plate was incubated 6 h, 25 ^{o}C, 5 % CO_2 before adding 100 μl PBS and centrifuging (5 min, 4 ^{o}C, 150x*g*). After removing the supernatant fraction, the wells were washed with 200 μl $well^{-1}$ of PBS, and centrifuged again. The supernatant fraction was removed and the cells were resuspended in 200 μl SDMEM containing 1× binding buffer (0.01M HEPES, 0.14 mM NaCl, 2.5mM $CaCl_2$) with or without annexin V-FITC (3.75 μl $well^{-1}$) and/or PI (0.5 μl $well^{-1}$). The autofluorescent background control did not receive annexin V-FITC or PI. The single positive PI control did not receive annexin V-FITC. The single positive FITC control did not receive PI. All other samples received both annexin V-FITC and PI. Samples were incubated for 5 min at RT and transferred to flow cytometry tubes containing 150 μl of FACS Flow sheath buffer containing 1× binding buffer. Samples were kept on ice protected from light and analyzed immediately by flow cytometry.

Caspase assay

Caspase activation was measured using a Vybrant® FAM Caspases Assay Kit (FITC) (Invitrogen/Molecular Probes) according to the manufacturer's instructions. This assay utilized a fluorescent inhibitor of caspases known as FLICA™

which detects activation of caspase enzymes in cells undergoing apoptosis. Using a 96-well, V-bottom plate, 1 x 10^5 coelomocytes in 0.1 ml SDMEM were added to appropriate experimental (H_20_2-treated) and control [untreated (0 mM) double negative autofluorescent background; single positive FITC; single positive PI; double positive caspase background] wells in duplicate. Experimental wells received 50 μl H_20_2 (final concentrations of 33.8 mM for EW F1-F3; 16.9 mM, 33.8 mM and 67.9 mM for EW F4-F6); single positive PI control wells received 50 μl 0.03 % saponin in SDMEM; and single positive FITC control wells received 50 μl SDMEM. All control and experimental samples were incubated for 6 h, 25 °C, 5 % CO_2. After centrifugation at 150x*g* (5 min, 4 °C), the supernatant fraction was removed and the wells were washed with 200 μl PBS. Again the plate was centrifuged and the supernatant fraction was removed. Untreated double-negative, autofluorescent control samples (FITC negative, PI negative) and single positive PI controls were resuspended in 100 μl of SDMEM. Untreated samples (caspase background) and H_20_2-treated samples were resuspended in 90 μl SDMEM plus 10 μl of 10X FLICA reagent. Single positive FITC control wells were resuspended in 50 μl SDMEM, 10 μl of 10X FLICA reagent, and 40 μl of 10 % formaldehyde. The plate was incubated in the dark, 1 h, 25 °C, 5 % CO_2, with gentle mixing every 20 min before adding 100 μl of 1× washing buffer and centrifuging as above. After removing the supernatant fraction, the cells were washed twice with 200 μl $well^{-1}$ of 1× wash buffer. Following the last centrifugation and removal of the supernatant fraction, 200 μl $well^{-1}$ of 1× wash buffer with or without PI was added to each well; double-negative and single positive FITC controls did not receive PI, all other samples received PI. Samples were placed on ice protected from light and analyzed immediately by flow cytometry.

Cell volume measurements

EW F4-F6 used in the caspase assay were also subjected to cell volume analysis using flow cytometry. Forward scatter measurements of PI-negative large coelomocytes treated in duplicate with 0, 16.9, 33.8 and 67.6 mM H_20_2 were averaged and analyzed by Student's t test to determine if differences observed in forward light scatter measurements were statistically significant compared to controls.

Flow cytometry

Fluorescence was measured using FL-1 (FITC, GFP and rhodamine 123) and FL-2 (PI) detectors of a FACSCalibur flow cytometer (BD Biosciences). Autofluorescent controls were used to set voltages for forward scatter (FSC), side scatter (SSC), FL-1 and FL-2 during instrument set-up. Single positive FITC and PI controls were used to adjust compensation settings (spectral overlap removal) for annexin V and caspase assays. LISTMODE data was acquired and analyzed using Cell Quest (BD Biosciences) and WinList5.0 (Verity Software House) software. Only coelomocytes corresponding to the large coelomocyte population (phagocytosis assays) or large and small coelomocyte populations combined (annexin V and caspase assays), as determined by appropriate granularity and size, were gated for further analyses.

DNA fragmentation assay

DNA purification was carried out according to Hermann *et al.* (1994) with some modifications. Briefly, coelomocytes from ten individual earthworms were extruded and plated at 1.5 x 10^5 coelomocytes $well^{-1}$ in 200 μl. For each treatment, 10 wells were used (1.5 x 10^6 coelomocytes per treatment from 10 individual earthworms), one well for each earthworm extruded, and each earthworm exposed to all treatments of the assay. H_20_2 was added at 0, 8.4, 16.9 or 33.8 mM and then incubated at 30 °C, 5 % CO_2, 6 h. After the incubation period, the plate was centrifuged (150x*g*, 10 min, 4 °C), the supernatant was removed, and the cells were gently resuspended by vortexing. Then 40 μl of lysis buffer (1% NP-40, 20 mM EDTA, 50 mM Tris-HCl, pH 7.5) was added to each well before pooling the 10 wells (10 individual earthworms) for each treatment group into a single microcentrifuge tube and centrifuging the lysate at 1600x*g*, 5 min to pellet debris. The supernatant was transferred to a new tube and the pellet was re-extracted with 40 μl lysis buffer and respun. Supernatants were combined for each treatment group, and adjusted to 1 % SDS, 5 μg ml^{-1} RNAse (Fermentas Life Sciences) and incubated 2 h at 56°C before adding proteinase K (Fisher, BP1700-50) (2.5 μg ml-1) and incubating 2 h at 37 °C. Then 0.5 volume 7.5 mM ammonium acetate and 2.5 volume of absolute ethanol was added to precipitate the DNA. DNA pellets were collected by centrifugation (14,000x*g*), rinsed with ice cold 70 % ethanol and air dried. Pellets were resuspended in 21 μl TE (10 mM Tris-Cl, 1 mM EDTA, pH 8,0) at 37 °C, 5 min before adding 4 μl loading dye (6x Blue/Orange Loading Dye, Promega, G1881) containing 1:100 SYBR® Safe gel stain (10,000X concentration in DMSO, Invitrogen). Molecular weight markers (10 μl $well^{-1}$) (exACTGene, Fisher BioReagents, BP257110) containing SYBR® Safe gel stain (2 μl $well^{-1}$) and DNA samples from each treatment group were electrophoresed in a 1.5 % agarose gel containing 1:10,000 SYBR® Safe gel stain in 1 x TBE (89 mM Tris base, 89 mM boric acid, 2 mM EDTA, pH 8.3), 120V until first dye front was ~ 2 cm from bottom of gel. Gels were photographed using a Gel-Documentation System (Bio-Rad).

TUNEL assay

A Flow TACS Apoptosis Detection Kit (Trevigen, Inc.) was used according to the manufacturer's instruction except 150,000 cell ml^{-1} were used in 0.5 volume recommended, and optional PI was not included. Coelomocytes were incubated in 0.2 ml SDMEM for 12 h at 25°C, 5% CO_2 with or without H_2O_2 (33.8 mM) before washing and fixing the cells. Flow cytometry measured FL-1 signals from gated amoebocytes. Samples were run in duplicate and subjected to statistical analysis by Student's t test.

Phagocytosis: endogenous H_20_2 production

Bacteria were introduced to coelomocytes (50,000 per well in 96 V-bottom plate in duplicate) at a m.o.i. ranging from 10:1 to 1000:1. Following 90 min incubation at 30 ^oC, DHR 123 (Invitrogen, D-632, 1 mM stock in DMSO) was added (1 μM final, 1:1000). After 10 min incubation at RT, samples were placed on ice, protected from light, and run on the flow cytometer immediately. Negative controls (no DHR 123) were incubated with 1:1000 DMSO to control for carrier effect of DMSO. Fluorescence was measured using the FL-1 detector.

Statistical Analysis

Data analysis and graphs were generated using Microsoft Excel 2007. The Student's t-test assuming unequal variance was utilized with a 95 % confidence interval to determine if the experimental values were statistically significant as exhibited as a p-value less than or equal to 0.05. All data is based on averages of either triplicate (exogenous H_20_2/phagocytosis and annexin V assays) or duplicate (endogenous H_20_2/phagocytosis, caspase and TUNEL assays) samples.

Results

Flow cytometry: exogenous phagocytosis assay

Figure 1 illustrates how our data was collected and analyzed to determine specific phagocytosis by hyaline amoebocytes from *E. hortensis* when using exogenous H_20_2. The left panel of the top row is a dot plot representing a typical coelomocyte profile obtained on the flow cytometer when analyzing forward scatter (FSC) (abscissa) versus side scatter (SSC) (ordinate) properties of earthworm

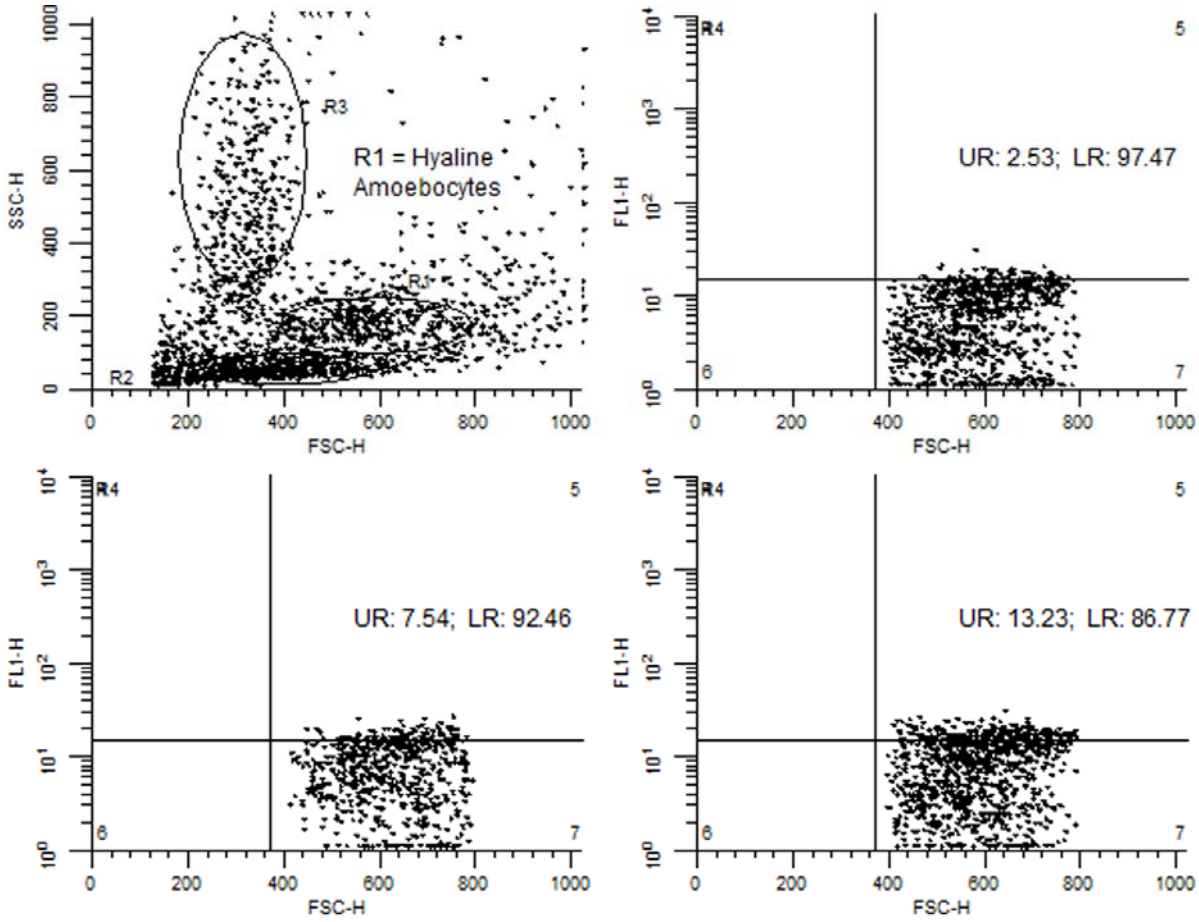

Fig. 1 Representative flow cytometry profile from phagocytosis assays. Top row: left panel shows a typical coelomocyte profile of FSC (size) (abscissa) versus SSC (granularity) (ordinate) of extruded earthworm coelomocytes where R1 = hyaline amoebocytes, R2 = granular amoebocytes, and R3 = eleocytes; right panel shows FSC (abscissa) versus FL-1 (relative fluorescence intensity) (ordinate) of R1-gated, untreated coelomocytes cultured without *E. coli*/GFP. Bottom row: FSC (abscissa) versus FL-1 (ordinate) of R1-gated coelomocytes cultured with *E. coli*/GFP without pretreatment (left panel) and with pretreatment (right panel) of H_20_2. FSC = forward scatter; SSC = side scatter; FL-1 = relative fluorescence intensity of GFP; UR = upper right; LR = lower right.

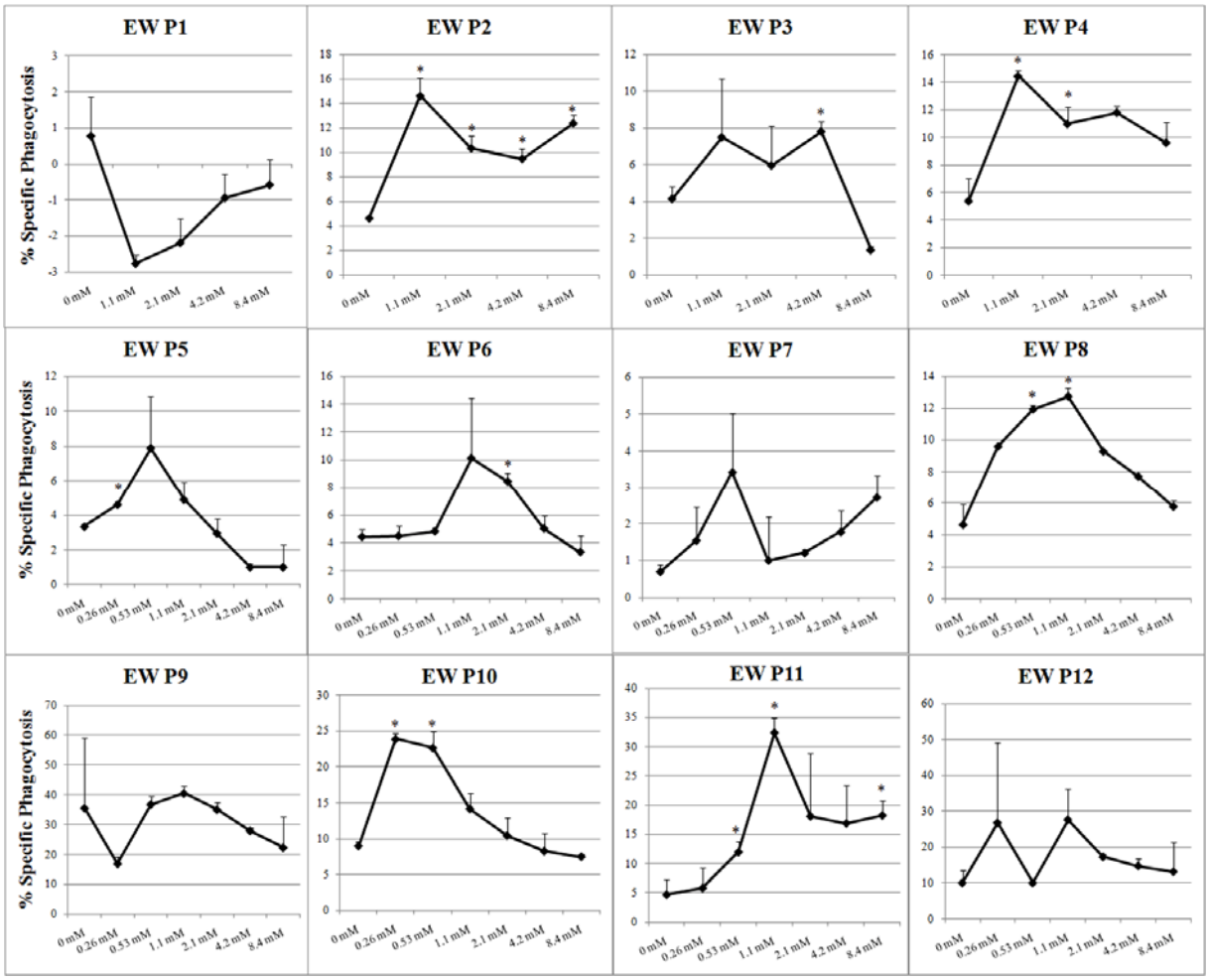

Fig. 2 Phagocytosis is enhanced by pretreating earthworm coelomocytes with H_20_2. Asterisks indicate $p \leq 0.05$. Top row: Earthworms EW-P1 – EW-P4 were pretreated with 0, 1.1, 2.1, 4.2 and 8.4 mM H_20_2. Middle and bottom rows: Earthworms EW-P5 – EW-P12 were pretreated with 0, 0.26, 0.53, 1.1, 2,1, 4.2 and 8.4 mM H_20_2.

coelomocytes. R1 depicts large coelomocytes (hyaline amoebocytes), R2 depicts small coelomocytes (granular amoebocytes), and R3 depicts chloragocytes (eleocytes). For analysis purposes and the determination of percent specific phagocytosis, FSC (abscissa) versus FL-1 (ordinate) dot plots were gated on hyaline amoebocytes (R1), the phagocytic cell population. The FSC versus FL-1 dot plots were partitioned into quadrants moving the horizontal bar (left to right) such that all of the events fell within the two right quadrants. The vertical bar (up and down) for FL-1 was established based on the negative control population (i.e., autofluorescence). Relative fluorescence intensity values for FL-1 delineate positive events (upper right quadrant - UR) and negative events (lower right quadrant - LR). The right panel of the top row shows FSC versus FL-1 for an untreated sample in the absence of *E. coli*/GFP, the negative control population. Note that the vertical bar was placed above the majority of events. The left panel of the bottom row shows an untreated sample in the presence of *E. coli*/GFP, while the right panel of the bottom row shows an H_20_2-treated sample in the presence of *E. coli*/GFP. Note the shift of the coelomocyte population from the LR (negative events) to the UR (positive events) quadrants between these two dot plots as fluorescence intensity increases due to phagocytic uptake of *E. coli*/GFP when pretreated with H_20_2. In this example percent positive events in UR increases from 7.54 to 13.23 % when coelomocytes were pretreated with H_20_2.

Effects of exogenous H_20_2 on phagocytosis

Having established the data analysis protocol, we studied the effect of H_20_2 at concentrations ranging from 0.26 - 8.4 mM on the phagocytosis of *E. coli*/GFP by earthworm coelomocytes. Percent specific phagocytosis of *E. coli*/GFP was determined by subtracting the percent positive events (UR) of negative controls (absence of *E. coli*/GFP) in FL-1 from each of the experimental samples (presence of *E. coli*/GFP with or without H_20_2). The average of duplicates of controls (0 mM H_20_2) versus H_20_2-treated samples were plotted and statistical significance was determined using the Student's t test. Figure 2 displays the results obtained for

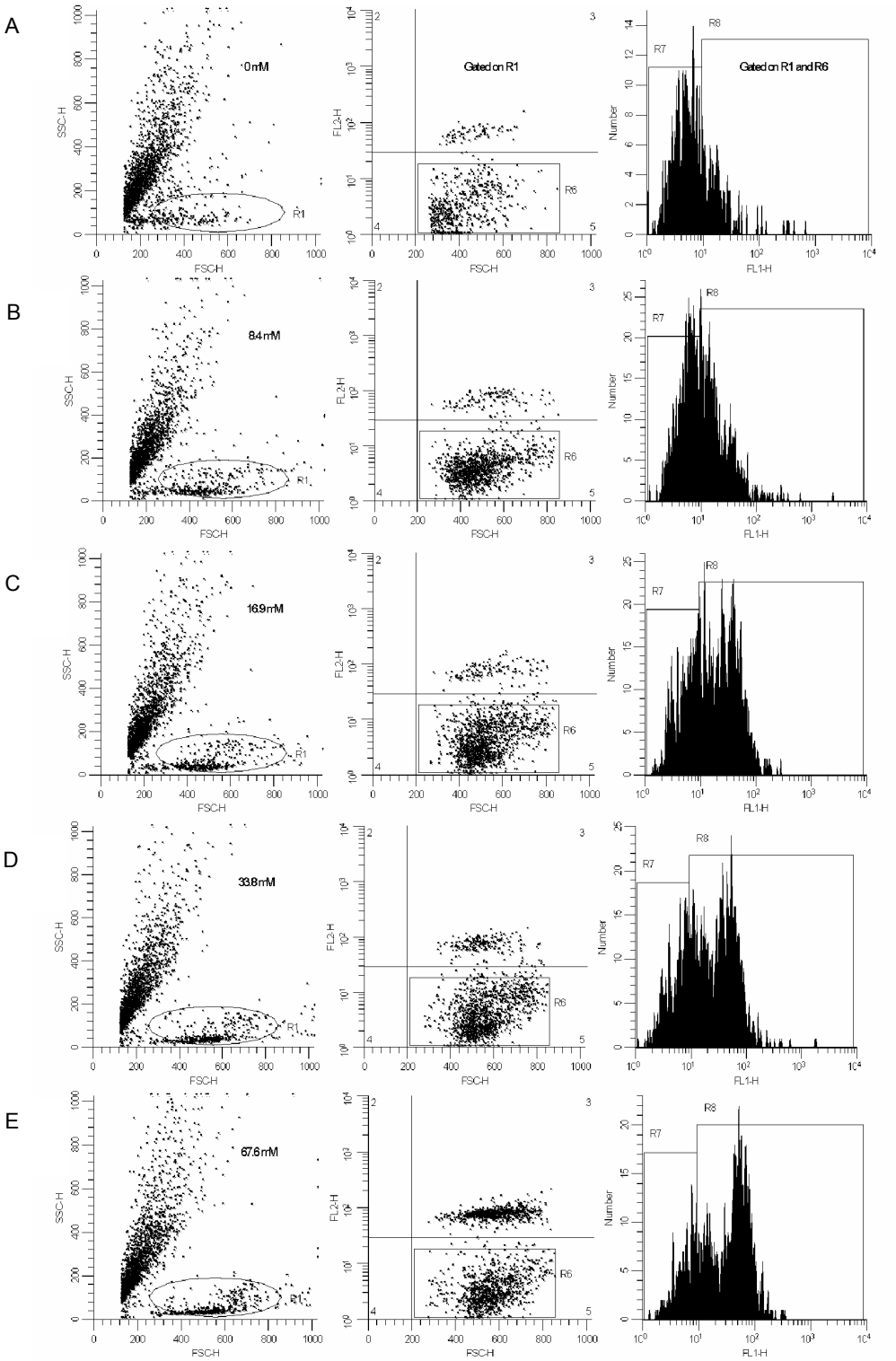

Fig. 3 Representative flow cytometry profile of annexin V-FITC/PI assay using EW-A7 as an example for data collection. Coelomocytes were pretreated with 0 (spontaneous apoptosis) (A), 8.4 (B), 16.9 (C), 33.8 (D) and 67.6 (E) mM H_20_2. Left hand column: FSC (abscissa) versus SSC (ordinate) of total, ungated coelomocytes population. Region 1 (R1) depicts the amoebocytes population (hyaline and granular amoebocytes). Middle column: FSC (abscissa) versus FL-2 (PI) (ordinate) of R1 gated amoebocytes (excluding eleocytes). Region 6 (R6) depicts PI-negative (FL-2 negative), viable amoebocyte population. Right hand column: FL-1 (abscissa) versus cell number (ordinate) of amoebocytes gated on R1 and R6 (i.e. only viable amoebocytes that have not taken up PI). Region 7 (R7) corresponds to annexin V negative amoebocytes while region 8 (R8) corresponds to annexin V positive (early apoptotic) amoebocytes. FSC = forward scatter; SSC = side scatter; FL-1 = relative fluorescence intensity of FITC, FL-2 = relative fluorescence intensity of PI.

Table 1 Percent early apoptotic cells binding annexin V-FITC in untreated and H_20_2-treated samples. Only cells residing in R1 and R6 were gated for annexin V-FITC analysis. R1 included hyaline and granular amoebocytes (not eleocytes) and R6 included PI-negative cells. Background autofluorescence of untreated samples not receiving annexin V-FITC or PI was subtracted from all values for each indicated earthworm sample before averaging triplicate data and performing statistical analyses. Results indicate data obtained from two assays performed by two independent researchers. Percent positive values for annexin V-FITC (± SD) are shown for spontaneous apoptosis (0 mM H_20_2) and two-fold serial dilutions from 67.6 to 8.4 mM H_20_2. Statistically significant values above spontaneous apoptosis levels are indicated as: * = $p \leq 0.05$; ** = $p \leq 0.005$; *** = $p \leq 0.0005$ as determined by Student's t test.

	Earthworm Sample	Spontaneous Apoptosis 0 mM	8.4 mM	16.9 mM	33.8 mM	67.6 mM
Assay 1	EW-A1	46.23 (±2.42)	31.75 (±1.33)	42.27 (±0.95)	62.81 (±2.39)***	82.86 (±1.48)***
	EW-A2	54.68 (±2.07)	52.82 (±0.74)	64.91 (±2.17)**	66.70 (±1.10)**	81.72 (±1.40)***
	EW-A3	31.76 (±1.67)	31.88 (±0.49)	39.51 (±1.13)**	49.99 (±1.26)***	62.03 (±1.45)***
	EW-A4	47.01 (±0.57)	36.99 (±1.22)	44.93 (±1.00)	49.78 (±5.04)	63.24 (±1.76)**
Assay 2	EW-A5	63.11 (±4.80)	50.40 (±0.96)	58.90 (±1.22)	79.79 (±2.35)*	85.99 (±0.67)*
	EW-A6	72.68 (±1.68)	69.51 (±0.63)	70.75 (±1.30)	71.56 (±2.65)	80.43 (±2.40)**
	EW-A7	31.95 (±0.51)	59.35 (±1.48)***	62.06 (±1.45)***	67.56 (±2.45)**	75.95 (±2.04)***
	EW-A8	38.75 (±2.25)	27.83 (±0.08)	27.25 (±1.23)	37.60 (±0.59)	46.88 (±1.12)*

coelomocytes from 12 earthworms pretreated *in vitro* with H_20_2 prior to phagocytosis. Earthworms 1, 2, 3 and 4 (EW-P1-P4) were pretreated in the range of 1.1 - 8.4 mM H_20_2, while EW-P5-P12 were pretreated in the range of 0.26 - 8.4 mM H_20_2. Eight of the 12 earthworms tested (67 %) exhibited statistically significant enhancement of phagocytosis to at least one of the concentrations employed. At doses above 8.4 mM, inhibitory effects on phagocytosis were observed (data not shown).

Flow cytometry detection of early apoptosis

For the next two experiments, which were aimed at investigating the effects of H_20_2 on PS translocation and caspase activation in amoebocytes of *E. hortensis*, it was important to be able to discriminate between necrotic/late apoptotic amoebocytes and amoebocytes undergoing early apoptosis to ensure that analyses were restricted to amoebocytes with intact plasma membranes. To do this, we utilized PI in addition to the fluorescein-tagged reporters of PS translocation and caspase activation. PI exhibits a sufficiently large Stokes shift compared to the fluorescein permitting simultaneous detection of fluorescein-labelled moieties and nuclear DNA providing the appropriate optical filters and compensation adjustments for spectral overlap are utilized. In our case, we used a FACSCalibur flow cytometer which employes FL-1 for fluorescein detection and FL-2 for PI detection. PI is membrane impermeant and is thus excluded from viable cells, making this fluorescent counterstain an ideal marker for identifying necrotic/late apoptotic cells in a population when used together with a second fluorescent dye which has minimal spectral emission overlap. Figure 3A illustrates the gating strategy used for the analysis of both the PS translocation and caspase activation experiments. First the coelomocytes were analyzed for FSC versus SSC (Fig. 3A - left panel) and region (R1) was set around the amoebocytes. Next a dot plot of FSC versus FL-2 gated on the R1 population was created and quadrants were established according to procedure described in Fig. 1 (Fig. 3A - middle panel) positioning the vertical bar at a location that clearly delineated live from dead cells based on the saponin-treated, PI-stained single-positive control employed for compensation purposes. The quadrants corresponded to regions 2-5 (R2-R5). Next another region (R6) was drawn around the PI-negative cell population, serving to identify viable cells (this would include non-apoptotic, non-necrotic and early-apoptotic cells whose membranes were still intact). Finally, a single parameter histogram measuring fluorescein (FL-1) was generated and gated on R1 (amoebocytes) and R6 (PI-negative cells). Therefore, only events that satisfied both prerequisites of belonging to the amoebocytes pool (hyaline and granular) as well as being viable were quantified in the R1/R6 gated FL-1 histogram (Fig. 3A - right panel). This strategy permitted the exclusion of necrotic/late apoptotic cells from the final analysis.

Table 2 Relative fluorescence intensity (RFI) of early apoptotic, annexin V-FITC-positive cells in untreated and H_20_2-treated samples. Only cells residing in R1 and R6 were gated for annexin V analysis. R1 included hyaline and granular amoebocytes (not eleocytes) and R6 included PI-negative cells. Triplicate data was averaged and subjected to statistical analyses. Results indicate data obtained from two assays performed by two independent researchers. RFI values (geometric mean) above background detected by FL-1 (± SD) are shown for spontaneous apoptosis (0 mM H_20_2) and two-fold serial dilutions from 67.6 to 8.4 mM H_20_2. Statistically significant values exceeding spontaneous apoptosis levels are indicated as: * = $p \leq 0.05$; ** = $p \leq 0.005$; *** = $p \leq 0.0005$ as determined by Student's t test.

	Earthworm Sample	Spontaneous Apoptosis 0 mM	8.4 mM	16.9 mM	33.8 mM	67.6 mM
Assay 1	EW-A1	14.75 (±0.59)	10.65 (±0.42)	11.22 (±0.08)	14.03 (±0.66)	19.69 (±0.94)**
	EW-A2	11.99 (±0.16)	12.56 (±0.44)	12.58 (±0.02)*	13.91 (±0.21)***	21.66 (±1.50)**
	EW-A3	15.12 (±0.57)	10.72 (±0.48)	11.70 (±0.47)	13.53 (±0.57)	14.90 (±0.41)
	EW-A4	12.79 (±0.12)	10.19 (±0.06)	11.20 (±0.12)	13.33 (±0.53)	18.02 (±0.39)**
Assay 2	EW-A5	29.88 (±1.92)	17.81 (±1.46)	18.40 (±0.19)	30.45 (±3.50)	81.52 (±5.72)**
	EW-A6	25.55 (±2.74)	19.13 (±0.40)	22.40 (±0.70)	28.61 (±0.28)	45.16 (±1.65)**
	EW-A7	12.23 (±1.61)	14.46 (±0.24)	23.22 (±0.40)**	26.48 (±0.82)***	31.84 (±0.65)***
	EW-A8	10.31 (±0.18)	10.35 (±0.35)	11.72 (±0.75)*	13.58 (±0.56)**	19.37 (±2.04)*

PS translocation: annexin V-FITC binding

Cells undergoing early apoptosis can be easily identified using annexin V, an anticoagulant protein that exhibits a high degree of specificity for PS, and when conjugated to a reporter molecule, such as fluorescein isothiocyanate (FITC), can be used an indicator of early apoptosis. PS is a phospholipid that is normally retained on the inner leaflet of the plasma membrane, however, in cells undergoing apoptosis, it is translocated to the outer leaflet and is exposed on the surface of the cell. Once exposed on the surface, it is accessible to annexin V binding. Early apoptotic cells maintain the integrity of their plasma membrane and are thus impermeable to PI. We conducted experiments to determine the effect of H_20_2 on PS translocation. We treated coelomocytes with H_20_2 in the range of 0 to 67.6 mM and after washing incubated them annexin V-FITC and PI. Figure 3 illustrates a representative set of flow cytometry obtained for earthworm 7 (EW-A7). As the concentration of H_20_2 increased, the degree of PS translocation also increased (right panels). The left hand panels illustrate that H_20_2 affected the morphology of the coelomocytes; as H_20_2 concentration increased, granularity (SSC) decreased (note tightening of SSC signal on ordinate). The middle panels shows that H_20_2 induced cell necrosis/late apoptosis at 33.8 mM and above.

In two separate assays performed by two independent researchers on separate days, eight earthworms were analyzed. Tables 1-3 report the overall findings of these experiments. Table 1 shows % annexin V-FITC binding of viable amoebocytes; 100 % (8/8), 63 % (5/8), 38 % (3/8) and 12.5 % (1/8) exhibited statistically significant PS translocation when exposed to 67.6, 33.8, 16.9 and 8.4 mM H_20_2, respectively. Note that untreated amoebocytes exhibit signs of spontaneous apoptosis, perhaps attributed to a stimulus delivered during isolation and/or *in vitro* culturing. Table 2 illustrates the increase in relative fluorescence intensity (RFI) of annexin V-FITC compared to baseline controls; 88 % (7/8), 38 % (3/8), and 38 % (3/8) revealed statistically significant increases in annexin V-FITC levels on the cell surface of viable amoebocytes following exposure to 67.6, 33.8 and 16.9 mM H_20_2, respectively. There was no significant increase in RFI in any of the earthworms when exposed to 8.4 mM H_20_2. Table 3 reveals that necrosis/late apoptosis correlates with increasing concentration of H_20_2 but only at the highest concentrations used; 100 % (8/8) and 63 % (5/8) of samples had statistically significant increases of necrosis/cell death compared to controls when exposed to 67.6 and 33.8 mM H_20_2, respectively. No significant difference in necrosis/cell death was observed at concentrations of 16.9 and 8.4 mM H_20_2.

Caspase activation in coelomocytes

To detect the events associated with signal transduction in cells undergoing apoptosis, we measured the activation of caspases in coelomocytes exposed to H_20_2 by using a reporter reagent called FAM-VAD-FMK FLICA where 1) FAM is the carboxyfluorescein group which fluoresces and is detectable in the FL-1 detector of the flow cyometer, 2) VAD is the three amino acid (valine, alanine, aspartic acid) generic probe that binds to most caspases (including caspases -1, -3, -4, -5, -6, -7, -8, and -9) and 3) FMK is the fluoromethyl ketone moiety which anchors the FAM-VAD-FMK reagent

Table 3 Percent late apoptotic/necrotic cells in untreated and H_20_2-treated samples. Only cells residing in R1 were gated for PI analysis. R1 included hyaline and granular amoebocytes (not eleocytes). Triplicate data was averaged and subjected to statistical analyses. Results indicate data obtained from two assays performed by two independent researchers. Percent PI-positive cells detected by FL-2 (± SD) are shown for spontaneous apoptosis (0 mM H_20_2) and two-fold serial dilutions from 67.6 to 8.4 mM H_20_2. Statistically significant PI values exceeding spontaneous apoptosis levels are indicated as: * = $p \leq 0.05$; ** = $p \leq 0.005$; *** = $p \leq 0.0005$ as determined by Student's t test.

	Earthworm Sample	Spontaneous Apoptosis 0 mM	8.4 mM	16.9 mM	33.8 mM	67.6 mM
Assay 1	EW-A1	24.55 (±1.19)	18.47 (±2.07)	25.93 (±1.00)	39.12 (±1.57)***	58.95 (±1.07)***
	EW-A2	14.03 (±2.71)	10.79 (±0.39)	11.43 (±0.40)	12.48 (±1.13)	49.93 (±1.80)***
	EW-A3	25.03 (±2.09)	18.79 (±0.63)	19.70 (±0.72)	22.85 (±0.20)	44.87 (±0.44)**
	EW-A4	24.85 (±0.14)	19.43 (±1.80)	20.90 (±1.01)	29.75 (±10.7)	45.75 (±2.89)**
Assay 2	EW-A5	50.61 (±1.86)	34.53 (±1.39)	39.47 (±2.29)	54.49 (±2.26)*	72.34 (±1.07)***
	EW-A6	35.93 (±2.79)	34.84 (±1.62)	35.96 (±2.17)	43.69 (±2.22)*	52.78 (±3.94)**
	EW-A7	15.48 (±2.05)	11.34 (±1.15)	16.11 (±1.15)	21.15 (±1.47)*	45.75 (±1.71)***
	EW-A8	20.17 (±3.34)	20.76 (±0.31)	23.69 (±4.15)	29.33 (±1.34)*	57.27 (±1.23)***

to activated caspases in the cell via a covalent cysteine linkage. Unbound FAM-VAD-FMK reagent is washed from the cell while bound reagent is anchored in the cell and fluoresces during flow cytometry, hence enabling the detection of activated caspases in cells undergoing the initial stages of apoptosis. We tested six earthworms in two separate assays. Figure 4 shows the results of these assays where coelomocytes were pretreated with 0 (A), 16.9 (B), 33.8 (C) and 67.6 (D) mM H_20_2. The same strategy for excluding necrotic/late apoptotic cells described in Fig. 3 was used in these experiments, i.e., relevant cells used for analysis were obtained by gating R1 (amoebocytes) and R6 (PI-negative) positive coelomocytes (Fig. 4). A marked increase in necrosis/cell death was observed between 33.8 and 67.6 mM H_20_2 (Fig. 4C-D). Again we observed changes in cellular morphology (as detected by FSC versus SSC profiles) as the concentration of H_20_2 increased, particularly at 67.6 mM (Fig. 4, middle panels). Statistically significant increases in caspase activation were detected in 100 % (3/3) and 67 % (4/6) of samples exposed to 67.6 and 33.8 mM H_20_2, respectively (Fig. 5).

Morphological changes in coelomocytes

EW F4-F6 were subjected to further analysis to determine if morphological changes associated with a decrease in cell volume, another hallmark of cells undergoing apoptosis, was occurring in response to H_20_2 treatment. Treated and untreated coelomocytes incubated with FAM-VAD-FMK FLICA and PI (as described in caspase assay above) were gated to select for PI-negative (viable and early apoptotic), large coelomocytes. Gated cells were analyzed in a single-parameter histogram measuring forward light scatter (FSC). Duplicate samples were averaged and p values were determined by Student's t test. Figure 6 shows a decrease in cell volume; in all cases except one (16.9 mM H_20_2 for EWF5), decreases in cell volume of H_20_2-treated samples were statistically significant ($p < 0.05$) compared to untreated samples. The difference in cell volume was much more pronounced in the large coelomocytes (Fig. 6) than in the small coelomocytes (data not shown). These results show that in earthworms undergoing biochemical changes (caspase activation), morphological alterations (cell volume) are also occurring.

DNA fragmentation

Another hallmark of apoptosis is the fragmentation of DNA which occurs when an endonuclease (caspase-activated deoxyribonuclease, CAD) is activated as a consequence of programmed cell death induction. Genomic DNA is cleaved at sites between nucleosomes at ~ 200 base pairs (bp) intervals (Nagata, 2000). In this study, total coelomocytes (including amoebocytes and eleocytes) were pretreated with H_20_2 prior to the purification and electrophoresis of DNA. In the first assay (Fig. 7, right hand gel), H_20_2 was used at 0 and 33.8 mM. DNA fragmentation consistent with apoptosis was

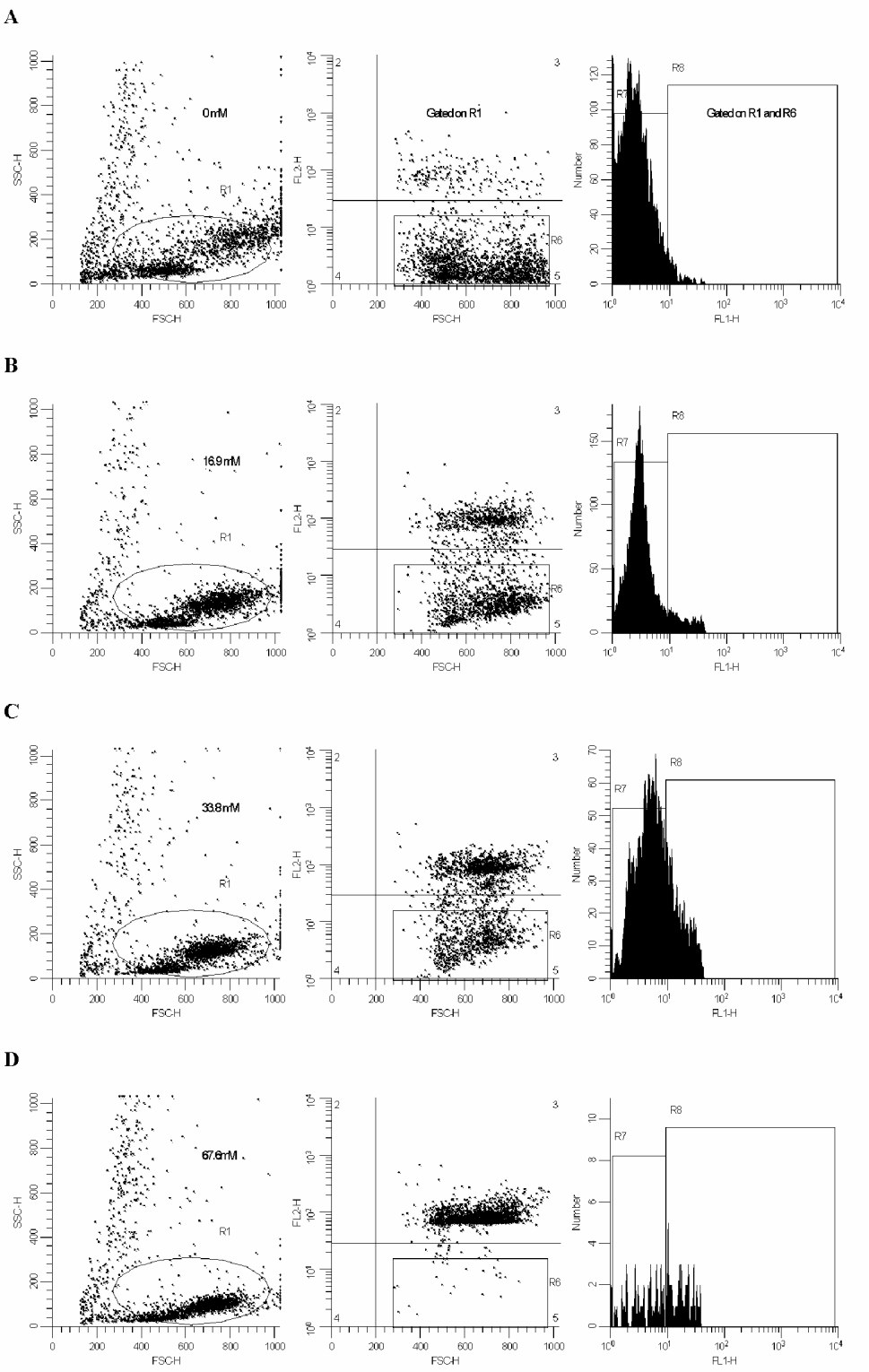

Fig. 4 Representative flow cytometry profile of caspase (FLICA/PI) assay using EW-F6 as an example for data collection. Coelomocytes were pretreated with 0 (spontaneous apoptosis) (A), 16.9 (B), 33.8 (C), and 67.6 (D) mM H_20_2. Left hand column: FSC (abscissa) versus SSC (ordinate) of total, ungated coelomocyte population. Region 1 (R1) depicts the amoebocyte population (hyaline and granular amoebocytes). Middle column: FSC (abscissa) versus FL-2 (PI) (ordinate) of R1 gated amoebocytes (excluding eleocytes). Region 6 (R6) depicts PI-negative (FL-2 negative), viable amoebocyte population. Right hand column: FL-1 (abscissa) versus cell number (ordinate) of amoebocytes gated on R1 and R6 (i.e. only viable amoebocytes that have not taken up PI). Region 7 (R7) corresponds to fluorescein negative amoebocytes while region 8 (R8) corresponds to fluorescein positive (early apoptotic) amoebocytes. FSC = forward scatter; SSC = side scatter; FL-1 = relative fluorescence intensity of fluorescein, FL-2 = relative fluorescence intensity of PI.

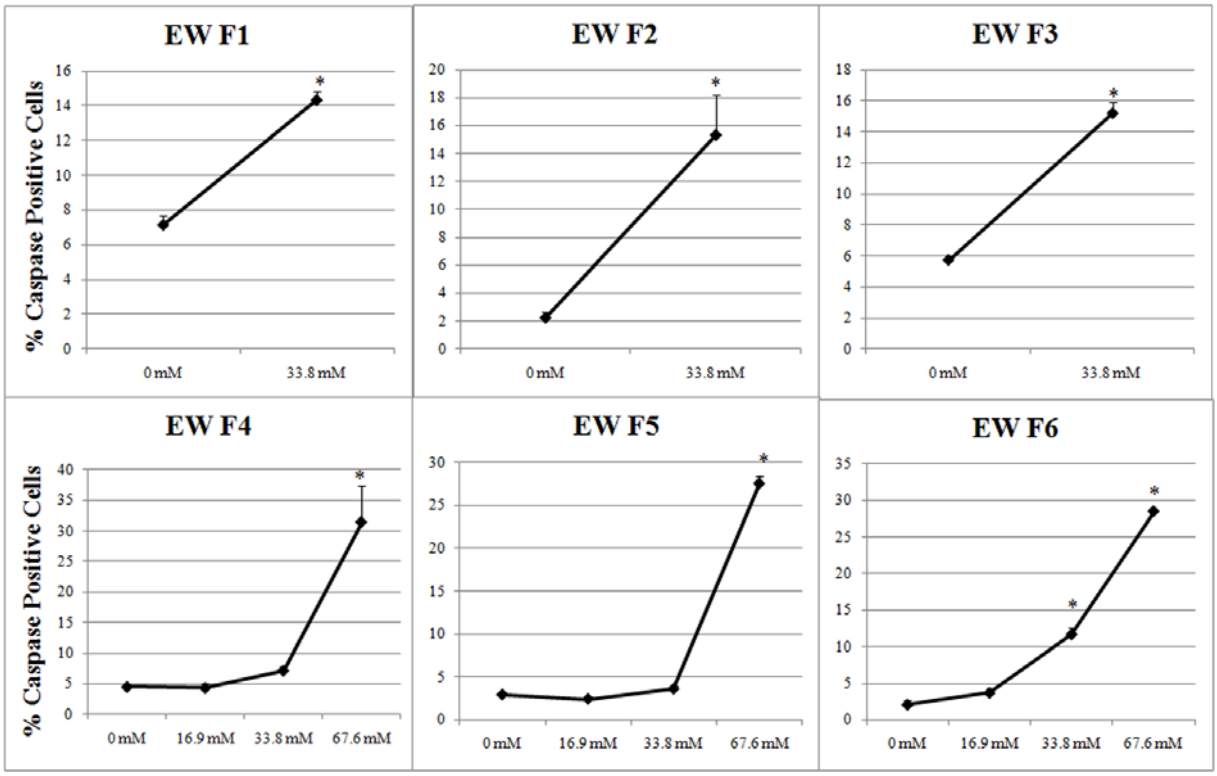

Fig. 5 Caspase activation in untreated and H_20_2-treated coelomocytes. Top row: Percent caspase positive amoebocytes of EW-F1-F3 treated with 0 mM (spontaneous apoptosis) or 33.8 mM H_20_2. Bottom row: Percent caspase positive amoebocytes of EW-F4-F6 treated with 0, 16.9, 33.8 and 67.6 mM H_20_2. Asterisks denote $p \leq 0.05$ compared to control.

observed compared to the untreated control. In a second assay (Fig. 7, two left hand gels) H_20_2 was used at 0, 33.8, 16.9 and 8.4 mM. Laddering was observed only when coelomocytes were exposed to 33.8 and 16.9 mM H_20_2. These results indicate that initiation of the stereotypical internucleosomal degradation of genomic DNA characteristic of apoptosis is occurring in earthworm coelomocytes in response to oxidative stress.

TUNEL assay

A terminal dUTP nick-end labeling (TUNEL) method was used to enzymatically verify DNA fragmentation in H_2O_2-treated coelomocytes. This method involved labeling the 3'-hydroxyl DNA ends generated during DNA fragmentation using a terminal deoxynucleotidyl transferase (TdT) and biotin-labeled UTP. Labeled DNA was detected by incubating with FITC-conjugated streptavidin and subjecting the samples to flow cytometric analysis. Amoebocytes identified on forward versus side scatter dot plots were gated for FL-1 (FITC) analysis. Four earthworms were treated with 33.8 mM H_2O_2, however, only three exhibited any demonstrable difference in labeling compared to untreated controls(EW T1, EW T2 & EW T4); two of these (EW T1 & EW T2) were statistically significant ($p < 0.006$). Figure 8 shows the results from the three responding earthworms. Note the increase in relative fluorescence intensity compared to untreated controls. A nuclease control was included for verification purposes (data not shown). These results complement the agarose gel electrophoresis results and illustrate that flow cytometry combined with the TUNEL assay is a useful and rapid method to detect DNA fragmentation in earthworm coelomocytes.

H_20_2 production during phagocytosis

Our final investigation was aimed at determining whether hyaline amoebocytes of *E. hortensis* undergo a respiratory burst and produce endogenous H_20_2 upon phagocytosis of the soil bacteria *P. stutzeri* (gram negative) and *B. megaterium* (gram positive). We used DHR 123, a fluorogenic molecular probe (excitation 505 nm; emission 534 nm) to detect the generation of H_20_2. DHR 123 is oxidized by H_20_2 and is converted consequently to it fluorescent derivative rhodamine 123, which can be measured intracellularly by the flow cytometer. Flow cytometry analysis involved: 1) setting a region around the hyaline amoebocytes (as described in Fig. 1, top row, left hand dot plot); 2) generating a FL-1, single-parameter histogram gated on this region; and 3) establishing a boundary (markers) to separate negative events from positive events (as described in Fig. 4, right hand histograms). The boundary was established based

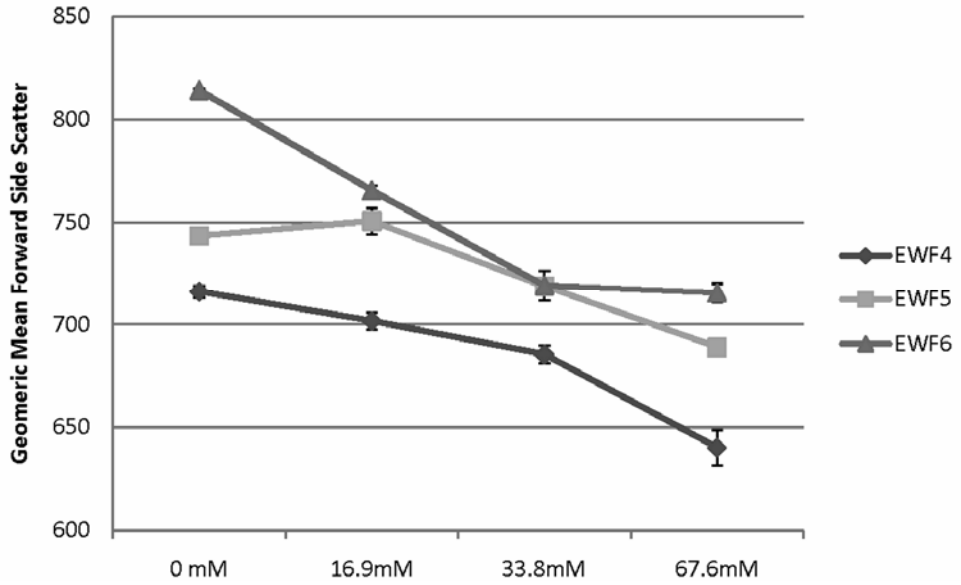

Fig. 6 Cell volume changes in untreated and H_20_2-treated coelomocytes. EW F4-F6 samples from the caspase assay were gated on PI-negative events falling in the region corresponding to the large coelomocyte population. H_20_2 concentration (abscissa) versus geometric mean of forward side scatter (ordinate) are plotted for EW F4 (diamonds), EW F5 (squares) and EW F6 (triangles). With the exception of EW F5 at 16.9 mM, p values < 0.05 compared to controls (untreated) were obtained.

on the negative control sample which was incubated in the absence of DHR 123 (but with an equivalent amount of DMSO compared to experimental samples) to control for autofluorescence. Any events exceeding the FL-1 boundary marker were considered positive (percent positive hyaline amoebocytes). Eight earthworms were extruded and three (EW 2, 7 and 8) were selected for the phagocytosis assay based on the quality of the coelomocytes (i.e., higher proportion of amoebocytes compared to eleocytes and adequate cell numbers). Figure 9 shows the results of these three earthworms and illustrates that DHR 123 is oxidized to rhodamine 123 during phagocytosis of *P. stutzeri* and *B. megaterium*. Statistical significance was determined based on comparison between control (DHR 123 only) and experimental (bacteria plus DHR 123) samples. *P. stutzeri* generated statistically significant results in 100 % and 67 % of cases at a m.o.i. of 100:1 and 10:1, respectively. *B. megaterium* generated statistically significant results in 67 % of cases at a m.o.i. of 100:1 and 10:1. A second assay employing *P. stutzeri* at a m.o.i. of 1000:1 revealed enhanced H_2O_2 production in 67% of cases (4 out of 6 earthworms) compared to controls (data not shown).

Discussion

This study demonstrates that exogenous H_20_2 (0.26 - 8.4 mM) caused an increase in phagocytosis by *E. hortensis*; 67 % of earthworms tested exhibited statistically significant enhancement of percent specific phagocytosis for one or more of the concentrations of H_20_2 used. Bejarano *et al.* (2007), Gamaley *et al.* (1994) and Takeda *et al.* (1998) examined the effects of oxygen free radicals in cultured human neutrophils, murine macrophages and rat ameboid microglia, respectively, and found that exposure to exogenous H_20_2 also caused an increase in phagocytic function. It is interesting to propose that in our model H_20_2 may be acting as a second messenger involved in evoking a significant elevation of phagocytic function. We are interested in determining if calcium mobilization from agonist-sensitive intracellular stores or influx across the plasma membrane accompanies H_20_2-enhanced phagocytosis, an effect reported by others (Redondo *et al.,* 2004; Bejarano *et al.,* 2007). The use of a calcium quelator (e.g., dimethyl BAPTA) would help to reveal the role, if any, that calcium mobilization plays in phagocytosis in earthworms, and to facilitate a better understanding of the physiological role of oxygen free radicals in calcium homeostasis. We also plan to examine the effect of pre-treating earthworm amoebocytes with catalase, an enzyme facilitating H_20_2 decomposition into water and oxygen, prior to the addition of exogenous H_20_2 in phagocytosis assays.

In parallel with the invertebrate studies of Blanco *et al.* (2005) which examined the effects of H_20_2 on coelomocytes of *Themiste petricola* (the sipunculan marine worm), we also revealed that H_20_2 induced apoptosis-like cell death in coelomocytes of *E. hortensis*. Using PI, we were able to discriminate between viable coelomocytes (nonapoptotic and early apoptotic) and nonviable coelomocytes (necrotic/late apoptotic); PI-positive cells were excluded from flow cytometric analyses due to DNA labeling. Note that eleocytes were not included in

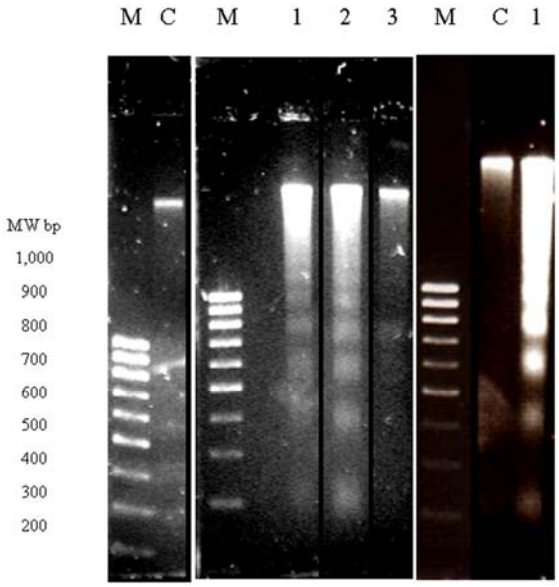

Fig. 7 DNA fragmentation of H_20_2-treated coelomocytes. These three gels represent two independent DNA fragmentation assays where earthworm coelomocytes were treated with H_20_2 for 6 h and DNA was isolated and electrophoresed in 1.5 % agarose gels in TBE buffer. Lanes M (molecular weight markers in bp are indicated for the nine distinct bands of the 100 bp ladder), Lanes C (untreated cells, 0 mM H_20_2), Lanes 1 (33.8 mM H_20_2), Lane 2 (16.9 mM H_20_2), and Lane 3 (8.4 mM H_20_2). The two left-hand gels are from the same assay and same population of coelomocytes. The right-hand gel is from a separate assay with a different population of coelomocytes.

these analyses owing to relatively high level of autofluorescence exhibited by this subpopulation. We observed PS translocation and caspase activation when amoebocytes were treated with H_20_2 in the range of 8.4 - 67.6 mM and 16.9 - 67.6 mM, respectively, under the conditions specified. It is interesting to note that relatively high concentrations of H_20_2 were required to induce apoptosis, suggestive of high TOSC in earthworm coelomocytes. We also observed dose-dependent changes in FSC when amoebocytes were pre-treated with H_20_2, a phenomenon consistent with apoptotic volume decrease (AVD) (Maeno *et al.,* 2000; Okada and Maeno, 2001) when cells undergoing apoptosis experience cell shrinkage and subsequent cell fragmentation (apoptotic bodies). Exposure of PS on the surface of infected coelomocytes may be one mechanism by which phagocytes recognize and remove cellular reservoirs of pathogens during innate immune responses. Fadok *et al.* (1992), for example, showed that murine macrophages rapidly recognize and remove apoptotic lymphocytes following exposure of PS on the outer leaflet of the plasma membrane of apoptotic cells, thereby prevent potential tissue damage from lysis of these cells *in vivo*.

Caspases are highly conserved and have been identified in invertebrates; for example the CED-3 protein of the nematode *Caehorhabditis elegans* was the first to be characterized. The gene encoding CED-3 is known to exhibit homology to murine and human caspase-1 (formerly known as interleukin-1 beta converting enzyme) (Yuan *et al.,* 1993). Several caspases known to participate in apoptosis have also been identified in *Drosophila melanogaster*

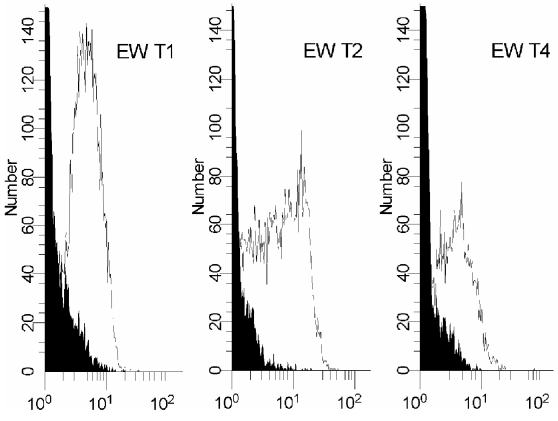

Fig. 8 TUNEL analysis of H_20_2-treated coelomocytes. Coelomocytes treated with 0 mM H_2O_2 (filled graph line) (control) or 33.8 mM H_2O_2 (unfilled graph line) were chemically fixed, and the fragmented DNA ends were labeled with biotin-conjugated UTP and stained with streptavidin FITC. The gated amoebocyte population was analyzed for FL-1 (FITC) fluorescence intensity (abscissa) versus cell number (ordinate). EW T1 and EW T2 exhibited statistical significance ($p < 0.006$) between untreated and treated amoebocytes.

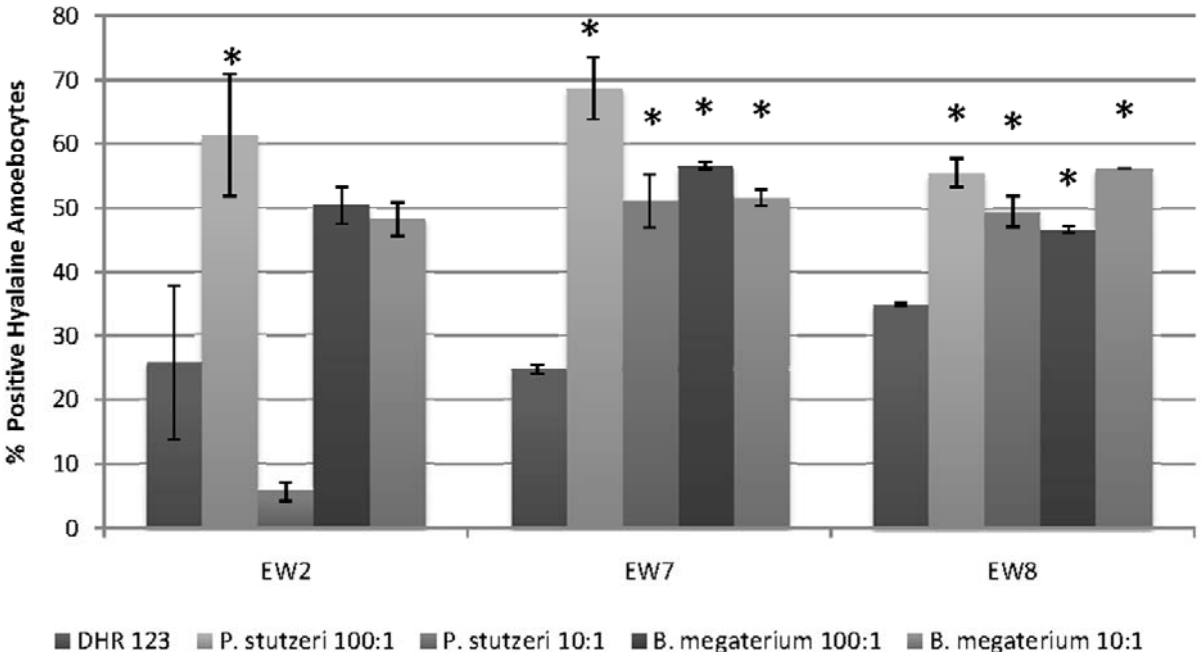

Fig. 9 Endogenous H_20_2 is produced during phagocytosis. The percent hyaline amoebocytes oxidizing DHR 123 to rhodamine 123 for each treatment is shown (percent positive hyaline amebocyes). Phagocytosis assays using *P. stutzeri* and *B. megaterium* at m.o.i. of 100:1 and 10: 1 compared to control (DHR 123) shows statistically significant ($p \leq 0.05$) increases in rhodamine 123 production (*) for EW 2, 7 and 8.

(reviewed in Boyce *et al.,* 2004). In addition, the crystal structure of Sf-caspase-1 from *Spodoptera frugiperda* has been resolved and its overall fold found to be exceedingly similar to active caspases from humans (Forsyth *et al.,* 2004). Using a fluorescent inhibitor of poly-caspases, our results show that H_20_2 induces caspase activation in earthworm amoebocytes. It would be worthwhile to try to dissect the caspase signaling pathway in *E. hortensis* using inhibitors known to target caspases with specificity for particular caspase subfamilies (Matsura *et al.,* 1999).

We also evaluated oligonucleosomal DNA fragmentation using agarose gel electrophoresis to resolve DNA fragments. A dose-dependent laddering pattern characteristic of apoptotic cells was observed when coelomocytes were treated with 16.9 and 33.8 mM, but not 8.4 mM H_20_2. Perhaps a longer incubation period would have resulted in DNA laddering at the lower concentration. The presence of discrete ~200 bp DNA fragments is consistent with apoptosis and not necrosis as the latter would result in random DNA fragmentation causing smears on an agarose gel rather than discrete repetitive oligonucleosomal fragments generated by endonuclease cleavage between nucleosomes (Walker *et al.,* 1988). In addition, we conducted TUNEL assays in conjunction with flow cytometry which provided enzymatic verification of DNA fragmentation in H_2O_2-treated coelomocytes, and a more rapid procedure for detecting DNA fragmentation in apoptotic cells. We are also interested in examining mitochondrial transmembrane potential using a mitochondria-specific probe such as JC-1 which incorporates into mitochondria and undergoes a shift in fluorescence emission spectra during membrane depolarization (Cossarizza *et al.,* 1995).

Finally, our results show that endogenous H_20_2 is produced by hyaline amoebocytes during phagocytosis of gram positive (*B. megaterium*) and gram negative (*P. stutzeri*) bacteria at m.o.i. ranging from 10:1 to 1000:1. Although further investigation is required *in vivo*, it is tempting to speculate that during infection in the earthworm, the production of H_20_2 facilitates physiological changes in coelomocytes that induce appropriate innate immune responses needed not only to eradicate pathogen load through ingestion (phagocytosis), but also to eliminate infected and damaged cells, and control cell numbers through a clearance mechanism (apoptosis). Engulfment of apoptotic cells would prevent the lytic release of toxic molecules (e.g. enzymes, proteases and oxidizing molecules) and spare or minimize surrounding tissue from inflammatory-type damage, thus enabling immune mechanisms to function effectively.

Acknowledgments
This work was funded by the Pennsylvania Academy of Science, the Beta Beta Beta National Biological Honor Society and the Cabrini College Science Department Research Fund.

References

Abele D, Tesch C, Wencke P, Pörtner, HO. How does oxidative stress relate to thermal tolerance in the Antarctic bivalve *Yoldia eightsi*? Antarct. Sci. 13: 111-118, 2001.

Adamowicz A, Wojtaszek J. Morphology and phagocytotic activity of coelomocytes in *Dendrobaena veneta (Lumbricidae*). Zoolog. Pol. 46: 91-104, 2001.

Axline SG, Reaven EP. Inhibition of phagocytosis and plasma membrane mobility of the cultivated macrophage by cytochalasin B; role of subplasmalemmal microfilaments. J. Cell Biol. 62: 647-659, 1974.

Bedard K, Krause K-H. The NOX family of ROS-generating NADPH oxidases: physiology and pathophysiology. Physiol. Rev. 87: 245-313, 2007.

Bejarano I, Terrón MP, Paredes, SD, Barriga C, Rodríguez AB, Parienta JA. Hydrogen peroxide increases the phagocytic function of human neutrophils by calcium mobilisation. Mol. Cell. Biochem. 296: 77-84, 2007.

Blanco GA, Bustamante J, Garcia M, Hajos SE. Hydrogen peroxide induces apoptotic-like cell death in coelomocytes of *Themiste petricola* (sipuncula). Biol. Bull. 209: 168-183, 2005.

Boyce M, Degterev A, Yuan J. Caspases: an ancient cellular sword of Damocles. Cell Death Differ. 11: 29-37, 2004.

Brenneisen P, Steinbrenner H, Sies H. Selenium, oxidative stress, and health aspects. Mol. Aspect. Med. 26: 256-267, 2005.

Cairo G, Tacchini L, Pogliaghi G, Anzon E, Tomasi A, Bernelli-Zazzera A. Induction of ferritin synthesis by oxidative stress. Transcriptional and post-transcriptional regulation by expansion of the “free” iron pool. J. Biol. Chem. 270: 700-703, 1995.

Coffey MD, Cole RA, Colles SM, Chisolm GM. In vitro cell injury by oxidized low density lipoprotein involves lipid hydroperoxide-induced formation of alkoxyl, lipid, and peroxyl radicals. J. Clin. Invest. 96: 1866-1873, 1995.

Cooper EL. Earthworm immunity. In: Invertebrate immunology. Rinkevich B, Műller WEG (eds), Springer Verlag, Heidelberg, pp 10-45, 1996.

Cossarizza A, Cooper EL, Quaglino D, Salvioli S, Kalachnikova G, Franceschi C. Mitochondrial mass and membrane potential in coelomocytes from the earthworm *Eisenia foetida*: studies with fluorescent probes in single intact cells. Biochem. Biophys. Res. Commun. 214: 503-510, 1995.

Cossarizza A, Cooper EL, Suzuki MM, Salvioli S, Capri M, Gri G, *et al*. Earthworm leukocytes that are not phagocytic and cross-react with several human epitopes can kill human tumor cell lines. Exp. Cell Res. 224: 174-182, 1996.

Cossarizza A, Pinti M, Troiano L, Cooper EL. Flow cytometry as a tool for analyzing invertebrate cells. Inv. Surv. J. 2: 32-40, 2005.

Csiszar A, Labinskyy N, Zhao X, Hu F, Serpillon S, Huang Z, *et al*. Vascular superoxide and hydrogen peroxide production and oxidative stress resistance in two closely related rodent species with disparate longevity. Aging Cell 6: 783-797, 2007.

Di Guilo RT, Washburn PC, Wenning RJ, Winston GW, Jewell CS. Biochemical responses in aquatic animals: a review of determinants of oxidative stress. Environ. Toxicol. Chem. 8: 1103-1123, 1989.

Dovzhenko NV, Kurilenko AV, Bel’cheva NN, Chelomin VP. Cadmium-induced oxidative stress in the bivalve mollusk *Modiolus modiolus*. Russian J. Marine Biol. 31: 309-313, 2005.

Dunford HB. Free radicals in iron-containing systems. Free Radic. Biol. Med. 3: 405-421, 1987.

Engelmann P, Pál J, Berki T, Cooper EL, Németh P. Earthworm leukocytes react with different mammalian specific monoclonal antibodies. Zoology 105: 257-265, 2002.

Engelmann P, Molnár L, Pálinkás L, Cooper EL, Németh P. Earthworm leukocyte populations specifically harbor lysosomal enzymes that may respond to bacterial challenge. Cell Tissue Res. 316: 391-401, 2004.

Engelmann P, Palinkas L, Cooper EL, Németh P. Monoclonal antibodies identify four distinct annelid leukocyte markers. Dev. Comp. Immunol. 29: 599-614, 2005.

Fadok VA, Voelker DR, Campbell PA, Cohen JJ, Bratton DL, Henson PM. Exposure of phosphatidylserine on the surface of apoptotic lymphocytes triggers specific recognition and removal by macrophages. J. Immunol. 148: 2207-2216, 1992.

Fato R, Bergamini C, Leoni S, Lenaz G. Mitochondrial production of reactive oxygen species: role of complex I and quinone analogues. BioFactors 32: 31-39, 2008.

Findlay VJ, Tapiero H, Townsend DM. Sulfiredoxin: a potential therapeutic agent?: Antioxidants in the prevention of human diseases. Biomed. Pharmacother. 59: 374-379, 2005.

Flohé L, Budde H, Hofmann B. Peroxiredoxins in antioxidant defense and redox regulation. Biofactors 19: 3-10, 2003.

Forman HJ, Torres M. Reactive oxygen species and cell signaling, respiratory burst in macrophage signaling. Am. J. Respir. Crit. Care Med. 166: S4-S8, 2002.

Forsyth CM, Lemongello D, LaCount DJ, Friesen PD, Fisher AJ. Crystal structure of an invertebrate caspase. J. Biol. Chem. 279: 7001-7008, 2004.

Fuller-Espie SL, Goodfield L, Hill K, Grant K, DeRogatis N. Conservation of cytokine-mediated responses in innate immunity: a flow cytometric study investigating the effects of human proinflammatory cytokines on phagocytosis in the earthworm *Eisenia hortensis*. Inv. Surv. J. 5: 124-134, 2008.

Gamaley IA, Kirpichnikova KM, Klyubin IV. Activation of murine macrophages by hydrogen peroxide. Cell. Signal. 6: 949-957, 1994.

Ghezzi P. Regulation of protein function by glutathionylation. Free Rad. Res. 39: 573-580, 2005.

Gorbi S, Regoli F. Total oxyradical scavenging capacity as an index of susceptibility to oxidative stress in marine organisms. Comments Toxicol. 9: 303-332, 2003.

Hartenstein V. Blood cells and blood cell development in the animal kingdom. Annu. Rev. Cell Dev. Biol. 22: 677-712, 2006.

Helfand SL, Rogina B. Genetics of aging in the fruit fly, *Drosophila melanogaster*. Annu. Rev. Genet. 37: 329-348, 2003.

Hermann M, Lorenz H-M, Voll R, Grünke M, Woith W, Kalden JR. A rapid and simple method for the isolation of apoptotic DNA fragments. Nucleic Acids Res. 22: 5506-5507, 1994.

Imlay JA. Pathways of oxidative damage. Annu. Rev. Microbiol. 57: 395-418, 2003.

Jankov RP, Kantores C, Pan J, Belik J. Contribution of xanthine oxidase-derived superoxide to chronic hypoxic pulmonary hypertension in neonatal rats. Am. J. Physiol. Lung Cell. Mol. Physiol. 294: L223-L245, 2008.

Kell DB. Iron behaving badly: inappropriate iron chelation as a major contributor to the aetiology of vascular and other progressive inflammatory and degenerative diseases. BMC Med. Genomics 2: 2, 2009.

Kalaç Y, Ayten K, Gűlruh U, Çotuk A. The role of opsonin in phagocytosis by coelomocytes of the earthworm *Dendrobaena veneta.* J. Cell Mol. Biol. 1: 7-14, 2002.

Kang JH, Kim KS, Choi SY, Kwon HY, Won MH. Oxidative modification of human ceruloplasmin by peroxyl radicals. Biochim. Biophys. Acta 1568: 30-36, 2001.

Larsen PL. Aging and resistance to oxidative damage in *Caenorhabditis elegans*. Proc. Natl. Acad. Sci. USA 90: 8905-8909, 1993.

Laukens D, Waeytens A, De Bleser P, Cuvelier C, DeVos M. Human metallothionein expression under normal and pathological conditions: mechanisms of gene regulation based on in silico promoter analysis. Crit. Rev. Eukaryot. Gene Expr. 19: 301-317, 2009.

Lewis DFV. Oxidative stress: the role of cytochromes P450 in oxygen activation. J. Chem. Tech. Biotechnol. 77: 1095-1100, 2002.

Livingstone, DR, Garcia Martinez P, Michel X, Narbonne, JF, O'Hara S, Ribera D *et al*. Oxyradical production as a pollution-mediated mechanisms of toxicity in the common mussel *Mytilus edulis* L, and other molluscs. Funct. Ecol. 4: 415-424, 1990.

Livingstone DR, Lemaire P, Matthews A, Peters LD, Porte C, Fitzpatrick PJ, *et al*. Assessment of the impact of organic pollutants on goby (*Zosterisessor ophiocephalus*) and mussel (*Mytilus galloprovincialis*) from the Venice Lagoon, Italy: biochemical studies. Mar. Environ. Res. 39: 235-240, 1995.

Loo G. Redox-sensitive mechanisms of phytochemical-mediated inhibition of cancer cell proliferation. J. Nutr. Biochem. 14: 64-73, 2003.

Maeno E, Ishizaki Y, Kanaseki T, Hazana A, Okada Y. Normotonic cell shrinkage because of disordered volume regulation is an early prerequisite to apoptosis. Proc. Natl. Acad. Sci. USA 17: 9487-9492, 2000.

Matsura T, Kai M, Fujii Y, Ito H, Yamada K. Hydrogen-peroxide-induced apoptosis in HL-60 cells requires caspase-3 activation. Free Radic. Res. 30: 73-83, 1999.

Mosiman V, Patterson B, Canterero L, Goolsby C. Reducing cellular autofluorescence in flow cytometry: an in situ method. Cytometry 30: 151-156, 1997.

Nagata S. Apoptotic DNA fragmentation. Exp. Cell Res. 256: 12-18, 2000.

Nordberg J, Arnér E.S.J. Reactive oxygen species, antioxidants, and the mammalian thioredoxin system. Free Rad. Biol. Med. 31: 1287-1312, 2001.

Okada Y, Maeno E. Apoptosis, cell volume regulation and volume-regulatory chloride channels. Comp. Biochem. Physiol. A 130: 377-383, 2001.

Panasenko OM, Osipov AN, Chekanov AV, Arnhold J, Sergienko VI. Peroxyl radical is produced upon the interaction of hypochlorite with tert-butyl hydroperoxide. Biochemistry 67: 880-888, 2002.

Patel M, Francis J, Cooper EL, Fuller-Espie SL. Development of a flow cytometric, non-radioactive cytotoxicity assay in *Eisenia fetida*: An *in vitro* system designed to analyze immunosuppression of natural killer-like coelomocytes in response to 7, 12 dimethylbenz[a]anthracene (DMBA). Eur. J. Soil Biol. 43S1:S97-103, 2007.

Pichaud N, Pellerin J, Fournier M, Gauthier-Clerc S, Rioux P, Pelletier E. Oxidative stress and immunologic responses following a dietary exposure to PAHs in *Mya arenaria*. Chem. Cent. J. 2: 23, 2008.

Raes MC, Toussaint O, Remacle J. Importance of Se-glutathione peroxidase, catalase, and Cu/Zn-SOD for cell survival against oxidative stress. Free Radic. Biol. Med. 17: 235-248, 1994.

Rattan SI. Theories of biological aging: genes, proteins and free radicals. Free Radic. Res. 40: 1230-1238, 2006.

Redondo PC, Salido GM, Rosado JA, Parienta JA. Effect of hydrogen peroxide on Ca^{2+} mobilisation in human platelets through sulphydryl oxidation dependent and independent mechanisms. Biochem. Pharmacol. 67: 491-502, 2004.

Regoli F. Total oxyradical scavenging capacity (TOSC) is polluted and translocated mussels: a predictive biomarker of oxidative stress. Aquatic Toxicol. 50: 351-361, 2000.

Sies H, Stahl W, Sundquist AR. Antioxidant functions of vitamins. Vitamins E and C, beta-carotene and other carotenoids. Ann. N. Y. Acad. Sci. 669: 7-20, 1992.

Strazzullo P, Puig JG. Uric acid and oxidative stress: relative impact on cardiovascular risk? Nutr. Metab. Cardiovasc. Dis. 17: 409-414, 2007.

Sundaram C, Koster W, Schallreuter U. The effect of UV radiation and sun blockers on free radical defence in human and guinea pig epidermis. Arch. Derm. Res. 282: 526-531, 1990.

Takeda H, Tomita M, Tanahashi N, Kobari M, Yokoyama M, Takao M, *et al*. Hydrogen peroxide enhances phagocytic activity of ameboid microglia. Neurosci. Lett. 240: 5-8, 1998.

Thannickal FJ, Fanburg BL. Reactive oxygen species in cell signaling. Am. J. Phsiol. Lung Cell. Mol. Physiol. 279: L1005-L1028, 2000.

Tyagi N, Sedoris KC, Steed M, Ovechkin AV, Moshal KS, Tyagi SC. Mechanisms of homocysteine-induced oxidative stress. Am. J. Physiol. Heart Circ. Physiol. 289: H2649-H2656, 2005.

Valko M, Rhodes, CJ, Moncol J, Izakovic M, Mazur M. Free radicals, metals and antioxidants in oxidative stress-induced cancer. Chem. Biol. Interact. 160: 1-40, 2006.

Walker NI, Harmon BV, Gobé GC, Kerr JF. Patterns of cell death. Methods Achiev. Exp. Pathol. 13: 18-54, 1988.

Wang G. NADPH oxidase and reactive oxygen species as signaling molecules in carcinogenesis. Front. Med. China 3: 1-7, 2009.

Yamaji Y, Nakazato Y, Oshima N, Hayashi M, Saruta T. Oxidative stress induced by iron released from transferrin in low pH peritoneal dialysis solution. Nephrol. Dial. Transplant. 19: 2592-2597, 2004.

Yuan J, Shaham, S, Ledoux S, Ellis HM, Horvitz HR. The *C. elegans* cell death gene ced-3 encodes a protein similar to mammalian interleukin-1 beta-converting enzyme. Cell 75: 641-652, 1993.